J|A|C|S
COMMUNICATIONS

Published on Web 06/10/2006

Oxide Hemostatic Activity

Todd A. Ostomel, Qihui Shi, and Galen D. Stucky*

Department of Chemistry and Biochemistry, University of California, Santa Barbara, California 93106

Received March 12, 2006; E-mail: stucky@chem.ucsb.edu

High-surface-area inorganic oxides are attractive materials for medical devices because of their mechanical integrity, tunable functionality, and resistance to phagocytosis and biological degradation.[1] Because most oxides have inherently polar surfaces, these materials are contact activators of the intrinsic pathway of the blood coagulation cascade.[2] The United States military, concerned because hemorrhage accounts for over 50% of battlefield casualties,[2] currently outfits soldiers with a porous and high-surface-area zeolite-based hemostatic agent (**HA**) designed to stabilize life-threatening hemorrhages by contact activation, dehydration, warming, and control of electrolytes in the wounded tissue.[3] In this report, the tunable in vitro hemostatic activity of high-surface-area hemostatic bioactive glass (**BG**) is evaluated by Thromboelastograph, a standard medical instrument for quantifying viscoelasticity changes of blood during thrombosis and fibrinolysis.[4] The hemostatic trends associated with hemostatic **BG**, and a new preparation of spherical hemostatic **BG**, along with similar Si- and Ca-containing oxides, are described and related to Si:Ca ratios, Ca^{2+} availability and coordination environment, porosity, $\Delta H_{Hydration}$, and surface area. Hemostatic **BG** is a new material with an excellent efficacy for inducing hemostasis and is chemically distinct from the traditional bioglass, a composite material developed by Hench and co-workers,[7] employed for bone growth.

Contact activation of blood, commonly referred to as the "glass effect", is the process by which polar surfaces activate the intrinsic pathway of the blood clotting cascade. It is also the underlying principle for the observation that blood tends to clot faster on glass surfaces than on plastic. The autocatalytic activation of clotting Factors XII, XI, prekallikrein, and high-molecular-weight kininogen is initiated by exposure of blood to a foreign polar surface, and this in turn activates the numerous feedback mechanisms responsible for the association of the thrombin enzyme and the polymerization of fibrin.[5] Essential to these chemical dynamics is surface area for immobilizing participants of surface-dependent clotting reactions and Ca^{2+} ions, which are cofactors that help to orientate protein assemblies and enzymes responsible for fibrin production (e.g., tenase complex).[6]

We identified hemostatic **BG** as an ideal inorganic **HA** because hemostatic **BG** will release Ca^{2+} ions upon hydration and is composed of an insoluble core that could provide an effective support for thrombosis. We have recently reported on the preparation of a related high-surface-area porous composite that demonstrates accelerated in vitro apatite growth when immersed in simulated body fluid.[8] We have extended this sol−gel synthetic preparation to include spray pyrolysis at 400 °C in a tube furnace to prepare the new spherical hemostatic **BG** (Supporting Information).

Thromboelastograph is an instrument used to diagnosis blood disorders by monitoring the change in viscoelasticity of blood during clot formation as a function of time.[9] A polyethylene cup, containing blood and a **HA**, is rotated ±5° about a torsion wire. The time until the bimodally symmetric viscoelasticity curve's amplitude is

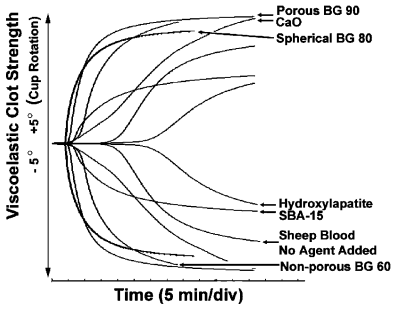

Figure 1. Oxide Thromboelastograph plots.

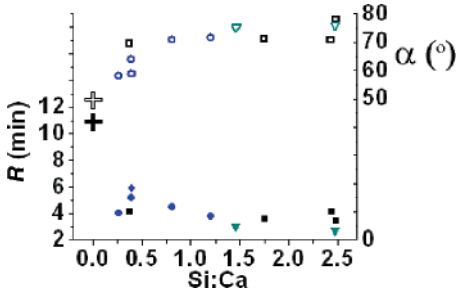

Figure 2. Plot of both clot detection time, *R* (filled shapes), and rate of coagulation, α (unfilled shapes), versus **BG** Si:Ca. Data represent the mean of four trials: ■ porous **BG**; ● nonporous **BG**; ▼ spherical **BG**; + no **HA**.

2 mm is referred to as *R* (min) and represents the initial detection of clot formation. The angle between the tangent to the curve and the horizontal is referred to as α (°) and is related to the rate of coagulation. The maximum separation of the curves is referred to as MA and represents the maximum clot strength (dyn/cm^2). An overlay of representative Thromboelastograph plots for the materials studied is shown in Figure 1.

The time until clot detection, *R*, decreases for increasing Si:Ca ratios in hemostatic **BG** (Figure 2). *R* is reduced by a factor of 2 when the Si:Ca ratio is doubled over the range studied. Hemostatic **BG** can perform the dual role of providing surface area for thrombosis and supplying Ca^{2+} ions; hence there will be an optimum ratio of SiO_2 to Ca^{2+} ions, which are cofactors throughout the clotting cascade[6,10] for the fastest hemostatic response. The hemostatic **BG**-induced coagulation rate, α, increases with increasing Si:Ca ratios and maximizes for the same Si:Ca ratio as for the minimum *R* time [Si:Ca($R_{min}\alpha_{max}$) ∼ 2.5]. All blood clots induced by hemostatic **BG**s resulted in stronger than natural clots, although there is no relationship between the ultimate clot strength and the ratio of Si:Ca for hemostatic **BG** ($MA_{BG} \geq 62$ and $MA_{Natural} = 58$ dyn/cm^2).

The rational design of composite oxide **HA**s requires an understanding of the thrombotic effects of the constituent oxides individually as well as collectively. Toward this end, we have analyzed the in vitro hemostatic activity of porous SiO_2 (SBA-15[11]) and CaO as model components of hemostatic **BG**, as well as nonporous SiO_2 glass beads (Polyscience, Inc. Cat #07666), $CaCO_3$,

10.1021/ja061717a CCC: $33.50

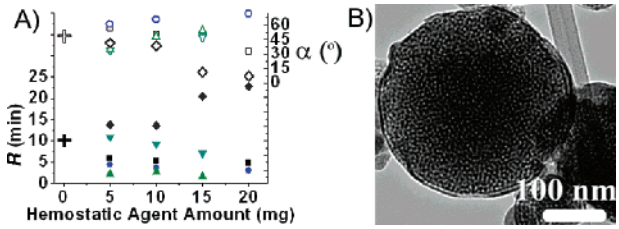

Figure 3. (A) Plot of both clot detection time, *R* (filled shapes), and rate of coagulation, α (unfilled shapes), versus Si:Ca. Data represent the mean of four trials: ■ SBA-15; ● glass beads; ▲ CaO; ▼ $CaCO_3$; ◇ hydroxylapatite; + no **HA**. (B) TEM of spherical **BG**.

and hydroxylapatite [$Ca_{10}(OH)_2(PO_4)_6$ Sigma Cat#289396] as related Si- and Ca-containing oxides. With the exception of hydroxylapatite, the synthetic analog of the oxide found in bone, each oxide demonstrated a reduced *R* time as more material was added to the blood (Figure 3A). The reduced rate of coagulation, α, and clot strength, MA, associated with adding hydroxylapatite to blood are also evidence of its anti-thrombotic capacity. While there are several reports of organic-based anticoagulants,[12] hydroxylapatite represents a unique inorganic oxide that delays coagulation.

Despite a reduction in the clot initiation time, both the rate and ultimate clot strength decreased as more SBA-15 was mixed with blood. Although SBA-15 is an initiator of contact activation, due to its hydroxylated surface and ability to concentrate blood by dehydration, it appears to inhibit the propagation of clot formation. This concentrating effect might be detrimental to clot propagation in the absence of sufficient Ca^{2+} near the concentrated blood. Glass beads, which can provide an activating hydroxylated surface without dehydrating blood, demonstrate both accelerated α and increased MA in addition to reduced *R* as more material was added. The dehydration of blood by porous hemostatic **BG** is not detrimental to clot propagation because Ca^{2+} ions are released near the concentrated blood. We found that the inclusion of Ca^{2+} ion sources with porous oxides, including SBA-15, assists rapid clot formation, and we are exploring the best incorporation methods.

Ca^{2+} ions are cofactors that play a critical role in the orientation of clotting enzymes on cellular surfaces[6] by serving as the ionic bridge between two negatively charged residues (e.g., cellular surface and clotting Factors). They are consumed during thrombosis and fibrinolysis when Factor XIII cross-links fibrin with negatively charged glycosylated residues. It is reasonable that the faster rates of coagulation and stronger clots attributed to both CaO and $CaCO_3$ are due in part to these agents' ability to present calcium to blood. CaO is far more soluble in blood (pH = 7.4) than $CaCO_3$, and the greater release of Ca^{2+} ions may account for the ≥30% stronger clots induced by CaO than those resulting from any of the other oxides discussed in this report, $MA_{CaO} = 92\ MA_{Other\ \mathbf{HA}s} \leq 66$. The difference in solubility between CaO and $CaCO_3$ appears to be a negligible factor with regard to the rate of coagulation.

Surface Ca species on undissolved **HA** particles could interact with clotting reactants in a fashion similar to that of Ca^{2+} ions that are coordinated to cellular surfaces,[13] and high-resolution X-ray photoelectron spectroscopic analysis demonstrates a lower Ca 2p binding energy for the faster clotting materials. Ca $2p_{3/2}$ in hydroxylapatite (349 eV) is 2 eV larger than that in hemostatic **BG**, CaO, or $CaCO_3$ (347 eV), in agreement with previous work.[14]

We observed that porous inorganic **HA**s have multiple accelerator effects on blood coagulation, in conjunction with surface activation and control of local electrolytes, by concentrating blood and locally warming the surrounding tissue due to an exothermic $\Delta H_{Hydration}$ common to porous oxides. Although the original porous zeolite **HA** employed by the U.S. military and civilian first-aid responders[15a] is effective as a life-saving medical device, the excessive heat generation led to efforts to identify new materials that will be safer to apply and still be effective.[9,15] The original zeolite-based **HA**s typically release up to 700 J/g upon hydration, adsorb ∼20% w/w H_2O, and have surface areas up to 600 m^2/g. Porous and nonporous hemostatic **BG**s release up to 400 J/g upon hydration, absorb ∼15% w/w H_2O, and have surface areas up to 400 m^2/g or greater. The smaller $\Delta H_{Hydration}$ for hemostatic **BG** permits local dehydration of hemorrhaging blood without the heat that inhibited proper application of the original zeolite-based **HA**.

We are studying the effect of particle morphology, and preliminary results indicate that size and shape are key clotting parameters. Spherical hemostatic **BG** was produced by spray pyrolysis of the **BG** precursor sol−gel (diameter = 300 nm, pore size = 5 nm) (Figure 3B). Given similar Si:Ca ratios, spherical hemostatic **BG** demonstrates reduced *R* times and faster coagulation rates than does irregular **BG**. Although both hemostatic **BG**s and zeolite **HA**s have high surface areas, the pore apertures (5 nm and 4 Å, respectively) restrict interaction with larger biological species to the outermost particle surface. Spherical hemostatic **BG** presents a more available surface to blood than irregular **BG**. Research is ongoing to explore the effect of the **HA**'s surface-to-volume ratio and the role of surface roughness and charge.

Acknowledgment. This work was funded by the Office of Naval Research, ONR Award N00014-04-1-0654, and made use the MRL central facilities supported by MRSEC Program of the National Science Foundation under Award No. DMR05-20415.

Supporting Information Available: Synthesis of **BG**, **HA**s, XPS, Thromboelastograph, thermal analysis, BET. This material is available free of charge via the Internet at http://pubs.acs.org.

References

(1) Ratner, B. D.; Hoffman, A. S.; Schoen, F. J.; Lemons, J. E. *Biomaterials Science: An Introduction to Materials in Medicine*, 2nd ed.; Elsevier: San Diego, CA, 2004.

(2) Ryan, K. L.; Kheirabad, B.; Klemke, H. G.; Martini, W.; Delgado, A. V.; Pusateri, A. E. *Army Medical Department Journal*, 2003, PB7−9, 12.

(3) Alam, H. B.; Chen, Z.; Jaskille, A.; Querol, R. I. L. C.; Koustova, E.; Inocencio, R.; Conran, R.; Seufert, A.; Ariaban, N.; Toruno, K.; Rhee, P. *J. Trauma* **2004**, *56*, 974.

(4) Salooja, N.; Perry, D. J. *Blood Coagulation Fibrinolysis* **2001**, *12*, 327.

(5) Halkier, T. *Mechanism in Blood Coagulation, Fibrinolysis, and the Complement System*; Cambridge University Press: Cambridge, NY, 1991.

(6) Hoffman, M. *J. Thromb. Thrombolysis* **2003**, *16*, 17.

(7) Hench, L. L. *J. Am. Ceram. Soc.* **1998**, *81*, 1705.

(8) Shi, Q.; Wang, J.; Zhang, J.; Fan, J.; Stucky, G. D. *Adv. Mater.* **2006**, *18*, 1038.

(9) Ostomel, T. A.; Stoimenov, P. K.; Holden, P. A.; Alam, H. B.; Stucky, G. D. *J Thromb. Thrombolysis* **2006**, in press.

(10) Xu, C.; Zeng, Y. J.; Gregerson, H. *Med. Eng. Phys.* **2002**, *24*, 587.

(11) Zhao, D.; Huo, Q.; Feng, J.; Chmelka, B.; Stucky, G. D. *J. Am. Chem. Soc.* **1998**, *120*, 6024.

(12) (a) Kogen, H.; Kiho, T.; Tago, K.; Miyamoto, S.; Fujioka, T.; Otsuka, N.; Suzuki-Konagai, K.; Ogita, T. *J. Am. Chem. Soc.* **2000**, *122*, 1842. (b) Lee, J.-C.; Lu, X.-A.; Kulkarni, S. S.; Wen, Y.-S.; Hung, S.-C. *J. Am. Chem. Soc.* **2004**, *126*, 476. (c) Espadas-Torre, C.; Oklejas, V.; Mowery, K.; Meyerhoff, M. E. *J. Am. Chem. Soc.* **1997**, *119*, 2321.

(13) Jalilehvand, F.; Spangberg, D.; Lindqvist-Reis, P.; Hermansson, K.; Persson, I.; Sandstrom, M. *J. Am. Chem. Soc.* **2001**, *123*, 431.

(14) (a) Perez-Pariente, J.; Balas, F.; Vallet-Regi, M. *Chem. Mater.* **2000**, *12*, 750. (b) Koper, O.; Lagadic, I.; Volodin, A.; Klabunde, K. *Chem. Mater.* **1997**, *9*, 2468.

(15) (a) Marshall, J. *New Scientist* **2006**, *2543*, 28. (b) Whang, H. S.; Kirsch, W.; Zhu, C. Z.; Hudson, S. M. *J. Macromol. Sci.* **2005**, *45*, 309. (c) Neuffer Marcus, C.; McDivitt, J.; Rose, D.; King, K.; Cloonan, C. C.; Vayer, J. S. *Mil. Med.* **2004**, *169*, 716.

JA061717A